Predicting the response of the Amazon rainforest to persistent drought conditions under current and future climates: a major challenge for global land surface models

E. Joetzjer[1], C. Delire[1], H. Douville[1], P. Ciais[2], B. Decharme[1], R. Fisher[3], B. Christoffersen[4], J.C. Calve[1], A.C.L. da Costa[5], L.V. Ferreira[6], P. Meir[7]

[1] *CNRM-GAME UMR3589, Groupe d'étude de l'atmosphère météorologique, Toulouse, France*
[2] *LSCE Laboratory of Climate Sciences and the Environment, Gif-sur-Yvette, France*
[3] *NCAR National Center for Atmospheric Research, Boulder, Colorado, USA*
[4] *School of GeoSciences, University of Edinburgh, Edinburgh, UK*
[5] *Universidade Federal de Para, Belem, Para, Brasil*
[6] *Museu Paraense Emilio Goeldi, Belem, Para, Brasil*
[7] *Australian National University, Canberra, Australia*

Abstract

While a majority of Global Climate Models project drier and longer dry seasons over the Amazon under higher CO_2 levels, large uncertainties surround the response of vegetation to persistent droughts in both present-day and future climates. We propose a detailed evaluation of the ability of the $ISBA_{CC}$ Land Surface Model to capture drought effects on both water and carbon budgets, comparing fluxes and stocks at two recent Throughfall Exclusion (TFE) experiments performed in the Amazon. We also explore the model sensitivity to different Water Stress Function (WSF) and to an idealized increase in CO_2 concentration and/or temperature. In spite of a reasonable soil moisture simulation, $ISBA_{CC}$ struggles to correctly simulate the vegetation response to TFE whose amplitude and timing is highly sensitive to the WSF. Under higher CO_2 concentration, the increased Water Use Efficiency (WUE) mitigates the $ISBA_{CC}$'s sensitivity to drought. While one of the proposed WSF formulation improves the response of most $ISBA_{CC}$ fluxes, except respiration, a parameterization of drought-induced tree mortality is missing for an accurate estimate of the vegetation response. Also, a better mechanistic understanding of the forest responses to drought under a warmer climate and higher CO_2 concentration is clearly needed.

Key words*: Amazon rainforest, drought, climate change, throughfall exclusion, land surface model, water stress functions.*

1. Introduction

The Amazon rainforest biome plays a crucial role in the global climate system regulating the regional energy, water and carbon cycles, and thereby modulating the tropical atmospheric circulation. The forest recycles about 25 to 35 % of the Amazonian precipitation through evapotranspiration (Eltahir et Bras, 1994) and stores about 10 to 15 % of the global above ground biomass (e.g. Potter 1999, Mahli et al., 2006; Beer et al., 2010; Pan et al., 2011).

The vulnerability of the Amazon forest to climate change is of great concern, especially as climate projections based on the fifth phase of the Coupled Model Intercomparison Project (CMIP5) show a between-model consensus towards dryer and longer dry seasons in this region (Fu et al., 2013; Joetzjer et al., 2013). Beyond this model consensus, however, substantial uncertainties in the current assessments given uncertainty in climate feedbacks and climate sensitivity to anthropogenic forcing remain. They arise from many sources including the limited ability of coupled ocean-atmosphere

general circulation models (OAGCMs) to capture the present-climate global patterns of temperature and precipitation as well as local vegetation-climate feedbacks (Jupp et al., 2010; Shiogama et al., 2011).

Land surface feedbacks also represent a significant source of uncertainties for climate projections over the Amazon basin (Meir et al., 2006; Friedlingstein et al., 2006; Poulter et al., 2009; Rammig et al., 2010; Galbraith et al., 2010; Booth et al., 2012). This was highlighted by the large spread in the future Amazonian evapotranspiration response to climate change among CMIP5 models (Joetzjer et al., 2013) and the growing evidence that global evapotranspiration has already been perturbed by human activities (Douville et al., 2013). About half of the CMIP5 models are Earth System Models (ESMs) that simulate the global carbon cycle and account for direct CO_2 effects on plants such as an increased water use efficiency (WUE) due to both photosynthesis (i.e. fertilization effect) and stomatal closure responses to increasing atmospheric CO_2 concentrations. Given the models' diversity and limited ability to capture biophysical mechanisms (e.g. Keenan et al., 2013), a process-oriented evaluation of the current-generation land surface models (LSM) is needed.

The Amazon forest is an ideal setting for evaluating land surface feedbacks in land surface models. The Amazon is projected to experience enhanced dry seasons in most CMIP5 climate scenarios, and possible though uncertain *dieback* of the Amazon rainforest in some projections (Cox et al., 2000; 2004; Galbraith et al., 2010; Good et al., 2013; Huntingford et al., 2013). Drought is likely to perturb biogeochemical cycles, stress vegetation, and disturb CO_2 fluxes and carbon stocks (van der Molen et al., 2011; Reichstein et al., 2013). For example, during the 2010 Amazonian drought, the net CO_2 uptake by a large area of the Amazon forest was reduced (Gatti et al., 2014). Severe droughts can also lead to tree damage, causing mortality and increased fire hazards (Nepstad et al., 2004; Phillips et al., 2009, 2010 ; Anderson et al., 2010), therefore reducing the carbon sink capacity of the Amazonian biome (Fisher et al., 2007; Mahli et al., 2008; Phillips et al., 2009; Lewis et al., 2011). Drying of the Amazon, coupled with higher temperatures and atmospheric CO_2 concentration, may have non-linear effects on water and carbon exchanges between soils, vegetation and the atmosphere (Berry et al., 2010).

The ability of land surface models to simulate response to drought can be tested using data from field experiments which manipulate precipitation inputs. Model validation was one aim of the two throughfall exclusion (TFE) experiments carried out in the eastern Amazon (at the National forest reserves of Tapajós and Caxiuanã, in eastern Amazonia) during the Large-Scale Biosphere-Atmosphere Experiment in Amazonia (LBA) (Nepstad et al., 2002; Meir et al., 2009; da Costa et al., 2010). Such field experiments are extremely useful to assess and improve the parameterization of hydrological, carbon and other ecosystem processes in LSMs (Galbraith et al., 2010; Sakaguchi et al., 2011; Powell et al., 2013). In particular, the simultaneous availability of soil moisture, sap flow and photosynthesis measurements provides a unique opportunity to evaluate the Water Stress Function (WSF) used in such models to represent the soil moisture effect on plants' stomatal conductance (Powell et al., 2013).

In this study, we evaluate how the $ISBA_{CC}$ Land Surface Model represents the vegetation response to persistent soil moisture deficit in both observed present-day and idealized future climates. First, we briefly describe the $ISBA_{CC}$ LSM developed at CNRM (Centre National de Recherches Météorologiques, Toulouse, France) and the in situ observations from the two TFE experimental sites (section 2). We then conduct a detailed evaluation of the ability of the $ISBA_{CC}$ LSM to capture drought effects on both water and carbon budgets, comparing fluxes and stocks at the TFE versus control sites (section 3). We explore the model sensitivity to the WSF parameterization and to an idealized increase in CO_2 concentration and/or temperature. Finally, we discuss the implications of our results for modeling the Amazon rainforest sensitivity to climate change (sections 4 and 5).

2 Model, observations and methods

2.1 $ISBA_{CC}$

2.1.1 Model description

The ISBA (Interaction Soil Biosphere Atmosphere) (Noilhan and Planton 1989; Noilhan and Mahfouf, 1996) Land Surface Model computes the exchanges of water and energy between the land surface and the atmosphere. In order to account for the interactions between climate and vegetation, Calvet et al. (1998) implemented a carbon assimilation scheme (A-gs). ISBA-A-gs does not explicitly account for enzyme kinetics but instead employs a semi-empirical response function which distinguishes between CO_2 and light-limited regimes, following the approach of Jacobs (1994).The effects of temperature on photosynthesis arise from the temperature dependencies of the CO_2 compensation point (Γ), mesophyll conductance (g_m), and the maximum photosynthetic rate ($A_{m,max}$) via standard Q_{10} response functions. The standard ISBA-A-gs equations describing these dependencies are given in Calvet et al., (1998) and Gibelin et al. (2006), and those relevant to the drought response are described in section 2.1.2. The A-gs scheme only accounts for the evolution of leaf assimilation and biomass. Gibelin et al. (2008) introduced a C-allocation scheme and a soil carbon module to represent the other pools and fluxes of carbon in the plant and in the soils. This latest version, called $ISBA_{CC}$ (ISBA Carbon Cycle) is used in this study. To better simulate soil moisture content in the deep Amazonian soils we use the multilayer soil diffusion scheme implemented in ISBA and described by Decharme et al. (2011; 2013). In addition, the canopy radiative transfer scheme developed by Carrer et al. (2013) is used.

The $ISBA_{CC}$ photosynthesis model relies on the concept of mesophyll conductance (g_m), also called internal conductance. As defined by Jacobs (1994), g_m quantifies the slope of the CO_2 response curve at high light intensity and low internal CO_2 concentration (C_i). It can be interpreted as a parameter to model the activity of the Rubisco under these conditions (cf. Table 1, Eq. 1). $ISBA_{CC}$ uses a constant unstressed value of g_m (g_m*) for each vegetation functional type (PFT). $ISBA_{CC}$ also defines a ratio f which relates C_i to ambient CO_2 (C_a) (Table 1, Eq. 2) that decreases linearly with increasing atmospheric humidity deficit (Table 1, Eq. 3). Assimilation is calculated from light, air humidity, C_a, the ratio f and finally, stomatal conductance (g_s) which measures gas (CO_2 and H_2O) exchange between the leaves and the atmosphere, is deduced from the assimilation rate. The sensitivity of g_m to the soil water availability is quantified by a water stress function (WSF), as explained below.

2.1.2 Water stress functions

The water stress function (WSF) is an empirical representation of the effect of soil moisture stress on transpiration and photosynthesis. In $ISBA_{CC}$, soil water content (SWC) affects transpiration and photosynthesis through changes in g_m and/or f_0 (Table 1), depending on the PFT and its drought strategy (Table 2). We test the two $ISBA_{CC}$ plant strategies (Fig. 1) proposed by Calvet et al. (2004): the *drought-avoiding* strategy (blue curve) for *isohydric* plants and the *drought-tolerant* response (purple) of *anisohydric* plants. One potential model limitation is that these parameterizations were derived from measurements made on saplings of *Pinus pinaster* and *Quercus petraea* (Picon et al., 1996), and have not been calibrated for mature trees or tropical species. In addition, we could not find experimental evidence for a direct effect of soil moisture on C_i that would support a function of f_0 = f(SWI) (Fig. 1, top right) and $ISBA_{CC}$-simulated photosynthesis and transpiration for tropical rainforests is highly sensitive to f_0, because the air is often close to saturation. Therefore, in addition to testing the existing WSF parameterizations, we also tested a linear WSF and the SiB3 formulation documented in Baker et al. (2008), both applied to g_m. These functions assume a

constant f_0 derived from in situ observations (Table 2, Domingues et al., 2007) and allow a larger stomatal conductance in line with a higher GPP and a higher evapotranspiration than the existing WSF functions in the model. The linear WSF describes plants that would reduce their stomatal conductance as soon as soil moisture drops below field capacity while the SiB3 WSF describes plants that would wait for drier soils before reducing their stomatal conductance. Despite a fairly similar response of g_m to soil moisture deficit between the linear and the drought tolerant WSF, and between the SiB3 and drought avoiding WSF, the linear and SiB3 WSFs induce a stronger response of g_s, LE and GPP to drought (Fig. 1) because f_0 is not a function of the soil moisture.

2.2 Site description and observations

Two rainfall exclusion experiments were initiated at Tapajós national forests (2.90°S 54.96°W) and Caxiuanã (1.72°S; 51.46°W) in 1999 and 2001 respectively. At each site, the experimental design consists of a 1 ha forest undisturbed control (CTL) and throughfall exclusion (TFE) plots in a nearby floristically and structurally similar forest plot. In the TFE plot, a portion of throughfall was excluded using large plastic panels below the canopy, approximately 1-2 m above the ground. A 1 m deep trench was dug around each plot to minimize lateral movement of water and roots. Panels were applied 1-yr after the beginning of the experiments to assess pre-treatment plot differences. At Tapajós (Caxiuanã), 1999 (2001) was the baseline year, and the TFE experiment lasted from 2000 until 2004 (2002 and remains ongoing). At Tapajós, panels were removed during the dry season (Fig 2) to reduce their influence on the forest floor through shading and heating. It was estimated that panels increased forest floor temperature by no more than 0.3°C (Nepstad et al., 2002). At Caxiuanã, panels were not removed because the risk of dry season storms is relatively high. The air temperature below the TFE panels was no different from ambient during the wet season, and varied up to 2°C warmer during the dry season; soil temperature differences in TFE remained similar to ambient throughout (Metcalfe et al., 2010).

While soils at both sites are highly weathered oxisols, they differ greatly in texture. Caxiuanã is a sandy soil and presents a stony laterite layer at 3 - 4m deep which could hamper deep roots development and soil water movement (Fisher et al., 2007), contrasting with the clay rich soil at Tapajós. Caxiuanã shows also a wetter climate (more precipitation and longer wet season) than Tapajós (Fig. 2) ; the water table depth reached 10 m at Caxiuanã during the wet season (Fisher et al., 2007)., but is below 80 meters at Tapajós (Nepstad et al., 2002).

Observations from the TFE experiments used to evaluate $ISBA_{CC}$ are summarized in Table 3. We use as a reference, evapotranspiration outputs from a 1-D model calibrated and validated at Tapajós from Markewitz et al., (2010, Table 5) and GPP estimated at Caxiuanã by Fisher et al., (2007) because there are no suitable direct measurements of water and carbon fluxes. The footprint of fluxtowers to 100 to 1000 times that of the experiments (Chen et al., 2008). Both fine-scale model outputs were carefully and successfully validated by the authors using datasets independent from those used to specify the model structure.

2.3 Simulations

At both sites, $ISBA_{CC}$ was run off-line using in situ hourly meteorological measurements made above the forest canopy at nearby weather stations. At Caxiuanã meteorological measurements were available for the entire experimental period (2001-2008), at Tapajós they covered only the years 2002 to 2004. To cover the entire period of experimentation, we cycled sequentially the available years. $ISBA_{CC}$ was run until the slowest soil storage pools of water and carbon had reached equilibrium.

$ISBA_{CC}$ explicitly simulates interception of precipitation by the canopy and throughfall as runoff

from the leaves. To simulate the experimental treatments at each site, we removed 60 % of the throughfall in our model runs. This is consistent with Markewitz et al., (2010) and Sakaguchi et al., (2011) for Tapajós, and similar to the 50 % exclusion of incident (above-canopy) rainfall implemented at Caxiuanã (Fisher et al., 2007; Galbraith et al., 2010; Powell et al., 2013). The 60 % reduction of throughfall was applied to the entire period at Caxiuanã (2001-2008) and only during the rainy seasons (January to June) from 2000 to 2004 at Tapajós, to mimic the experimental conditions.

At both sites, we imposed the 'evergreen tropical tree' plant functional type. To better represent soil moisture and focus on vegetation response, we constrained $ISBA_{CC}$ using the observed texture at each site. The soil texture values used for the simulations are, at Caxiuanã 75 % sand and 15 % clay (Ruivo and Cunha 2003) and 52 % sand and 42 % clay at Tapajós following the LBA-Data Model Intercomparison Project (www.climatemodeling.org/lba-mip). To mimic deep Amazonian soils, soil and root depth were fixed at 8 meters, even at Caxiuanã, because roots there were found below the laterite layer located at 3 – 4 m deep (Fisher et al., 2007). Representation of deep soil and roots may avoid the simulation of unrealistic responses to drought due to a drying of the upper layers (Baker 2008), although the sensitivity of soil moisture to soil depth may be small in soil diffusion models (Guimberteau et al., 2014). The same soil texture was used for all soil layers because of a lack of soil texture data for deeper depths, like the laterite layer at Caxiuanã. To represent the expected increase in bulk density in deeper soil layers, the hydraulic conductivity was assumed to increase exponentially with depth (Decharme et al., 2006).

Throughfall exclusion experiments are not fully representative of future climate conditions or atmospheric CO_2 concentrations. Besides more severe and persistent dry seasons, atmospheric CO_2 concentrations will increase as well as near-surface air temperature and VPD. Therefore we chose to analyze how the model sensitivity to drought can be affected by increased CO_2 concentration and increased temperature. In line with the idealized CMIP5 climate change experiments, we conducted simulations using the same TFE with arbitrary high values of CO_2 and temperature: four times the preindustrial CO_2 concentration (1080 ppmv), higher temperature (+4 °C), and a combination (Table 4). The CO_2 concentration and the increase in temperature are constant year round. We did not modify the specific humidity, but a 4°C arbitrary warming lowers the relative humidity and increases the evaporative demand of the atmosphere.

3 Results

3.1 Hydrological response

$ISBA_{CC}$ simulates the SWC and its seasonality fairly well between 0-3 m (Fig. 3) at both sites for the CTL plots, but the model tends to be too wet during the dry season. The low correlations (around 0.65) between observations and simulations at Tapajós are potentially due to the use of reconstructed forcing data, that was necessary to cover the entire experimental period. Despite a wetter climate (Fig. 2), the simulation at Caxiuanã produces a drier soil, in line with a sandier texture. Due to higher evapotranspiration, the SiB3 and linear WSF reduce the wet bias and improve the seasonality of simulated SWC. When throughfall exclusion is applied to the model, the observed reduction in SWC is also better captured by the linear and the SiB3 WSF (Fig. 3). The SWI remains close to one (field capacity) with the drought-avoiding and tolerant WSFs while it drops below 0.5 with the linear and SiB3 WSFs (Fig. 4). The unstressed transpiration fluxes (at SWI > 1) are lower with the drought-avoiding and tolerant WSFs and the soil moisture is not depleted quickly enough. Therefore, the edaphic water stress is not captured and we expect little impact on the vegetation fluxes. With the linear and SiB3 WSF, the stomatal conductance is much higher (Fig. 1, bottom left) and soil moisture is depleted much faster by transpiration. SWI clearly decreases,

imposing a strong hydrological stress, mainly with SiB3, as the SWI reaches values close to zero (the wilting point).

3.2 Vegetation response

3.2.1 Water and Carbon budget

To understand the response of $ISBA_{CC}$ to drought, we compare the density functions (Fig. 5) of daily SWI, g_s, GPP and LE for the dry (August to October) and the wet seasons (February to April). Only the drought-avoiding WSF is plotted because the drought-tolerant WSF showed a very similar behavior. The modeled values of g_s, LE and GPP are higher during the dry season than during the wet season in all control simulations, following the higher evaporative demand (Fig.1) due to higher available energy (less clouds) and little soil moisture stress (Fig. 4). The linear and SiB3 WSF have higher LE and GPP, due to higher stomatal conductance, and a stronger response to drought than using the drought-avoiding and tolerant WSFs. During a drought (dashed lines and shaded areas), the distribution of SWI is shifted towards lower values with the SiB3 and linear WSFs. With the tolerant (and avoiding) WSF, the simulated vegetation response to throughfall exclusion is weak ; SWI remains above 0.5 in all seasons, even during TFE.

At Caxiuanã, the reduction of SWI during TFE is more pronounced than at Tapajós, consistent with the sandier soil and the longer experiment. The strongest responses of the carbon and water fluxes happen during the dry season, when the soil moisture content drops close to wilting point revealing the high sensitivity to soil moisture content, and therefore to the seasonality in $ISBA_{CC}$. The response is more pronounced with the Linear and the SiB3 WSF than with the original functions, and, at Caxiuanã than at Tapajós.

All model simulations underestimate wet season stomatal conductance (g_s), which drives the water and carbon response to drought (Fig. 6). The dry season observations are better captured as all simulations are within the range of the observations, which themselves span a range of species, and thus show significant spread. Despite the wide observed g_s range, the response to drought is underestimated by all WSF except when soil moisture becomes extremely limited (TFE and dry season). The linear WSF shows the greatest response of g_s to drought.

Moving to annual fluxes (Fig. 7), for all water stress functions, $ISBA_{CC}$ simulates some decrease in LE and GPP between the CTL and TFE plots. The Linear WSF predicts a larger decline in LE and GPP, which is closer to observation-constrained estimates at both sites (Fisher et al., 2007; Markewitz et al., 2010). The SiB3 WSF allows a higher transpiration rate than the Linear function for the same intermediate SWC (Fig. 1), depleting the soil water faster, and giving a later but stronger response to drought at Caxiuanã. The linear and SiB3 WSF simulates the seasonal reduction in transpiration induced by throughfall exclusion reasonably well when compared to the measured daily sap flow (not shown).

3.2.2 Autotrophic and heterotrophic respiration

In comparison to ecosystem carbon fluxes derived by Metcalfe et al., (2010) at Caxiuanã, the model overestimates woody tissue respiration and underestimates respiration of leaves and roots. These errors compensate each other and overall the $ISBA_{CC}$ reasonably matches the yearly heterotrophic and autotrophic respiration fluxes (Fig. 8, CTL). This result remains valid over several sites across the Amazon watershed when comparing $ISBA_{CC}$ to the dataset compiled by Malhi et al., (2009) (not shown).

In contrast to the observations at Caxiuanã, $ISBA_{CC}$ predicts a decrease of the autotrophic

respiration with drought that is not balanced by the increase in vegetation temperature due to the decrease in latent heat production (which reaches a maximum of 2°C during the driest dry season). Whole ecosystem respiration was observed to increase during the TFE experiments mainly attributable to a temperature corrected enhanced leaf respiration rate per unit LAI (Metcalfe et al., 2010) as was observed during seasonal drought elsewhere in the Amazon (Miranda et al., 2005). One hypothesis to explain this observation is that the enhanced respiration may supply the supplementary energy demand induced by drought to actively maintain the gradients of the vacuolar solute to keep a minimum turgor (osmotic adjustment) and/or to repair water stress induced cell damage (Metcalfe et al., 2010; Atkin and Macherel 2009 and references within). The majority of ecosystem model, couple autotrophic respiration to assimilation, and implicitly to the LAI which declines during drought. In $ISBA_{CC}$ the heterotrophic respiration is a function of the soil water content, it decreases when in drought, contrary to observations.

3.2.3 Biomass carbon stocks

The simulated daily LAI compares reasonably well with the in situ observation at both control sites (Fig. 9). The SIB3 and linear WSFs result in LAIs a little higher than the drought-tolerant and avoiding WSFs (in line with a higher g_s and GPP, seen in Fig. 1). At Tapajós, $ISBA_{CC}$ underestimates LAI during the first years of the experiment (2000 to 2002), which might be partly explained by the reconstructed forcing for these years. At Caxiuanã the anomalously low LAI value (4 $m^2.m^{-2}$) measured in November 2002 is not captured by the model.

$ISBA_{CC}$ fails to simulate the observed substantial loss of LAI (from 1 to 2 points, about 20 % of leaf area, Meir et al., 2009) during TFE at both sites. With the drought-tolerant and avoiding WSFs, the soil water content remains above field capacity (SWI > 1, Fig. 4) at both sites, and the simulated LAI shows no response to drought. When using the linear or SiB3 WSF, the loss of LAI remains underestimated at Tapajós, where the SWI remains relatively high compared to Caxiuanã (Fig. 4). At Caxiuanã, the observed LAI in the TFE experiment diverged from the control within two years by more than one LAI unit. There are no LAI measurements between 2004 and 2007. The model underestimates the early LAI decrease consecutive to TFE in 2003 with all the WSFs. From the end of 2005 through 2007, the SiB3 WSF results in strong and rapid decreases of LAI during the dry seasons followed by rapid recovery during the wet seasons, partly driven by the the strong seasonality of the soil moisture which almost reaches the wilting point during each dry season after 2005 (Fig. 4).

Although there were no LAI observations in 2005 and 2006, it is likely that this four point decrease of simulated LAI is too strong, and the speed of the recovery is not realistic. The fast changes in modelled LAI (Fig 9) showing little memory of previous droughts are coherent with the model's hypothesis that the LAI is driven by current assimilation (Gibelin et al., 2006). With the linear WSF, the model's behavior is closer to reality because the SWC remains higher and the vegetation shows a smoother response to drought.

Above-ground biomass observations at Caxiuanã show a reduction of stand-level biomass by 20 % after seven years of TFE, mainly due to enhanced tree mortality. The model predicts AGB in the CTL plot with some skill, but the loss of AGB in the TFE is strongly underestimated with the Linear and SiB3 WSF, and not captured at all with the original WSF (Fig. 10). This result is not surprising since $ISBA_{CC}$ only represents background turnover rates depending on biomass stocks and fixed turnover times. There is no representation of mortality processes driven by plant physiology or strong climate anomalies.

3.3 Drought response sensitivity to background temperature and CO_2

Under a warmer climate (+4°C), the higher evaporative demand increases LE (Fig 11, top left panels black dots), and the model becomes more sensitive to drought (Fig 11, top left panels red dots). Conversely, LE is strongly reduced in the high CO_2 simulation due to increased water use efficiency (WUE), as expected because stomata need to be less open, therefore reducing transpiration, for the same CO_2 uptake (Woodward, 1987; Lloyd and Farquhar, 2008). Consequently, the model sensitivity to the experimental drought is completely dampened. The SWI remains close to or above 1 even when removing 60 % of the incoming throughfall (red dots).

The GPP is barely impacted by the +4°C in the CTL plot, as the temperature is already close to the assimilation optimum temperature, but is limited in the exclusion plot due to the stronger water stress linked with temperature-induced higher evaporation rates. Maximum GPP increases by about 50 % under 4x CO_2 because of the fertilization effect. It remains high in the TFE plot because the soil remains wet due to the reduction of transpiration. Under higher CO_2 concentration, the CO_2 diffusion into the mesophyll is easier, therefore enhancing the carboxylation rate (Lloyd and Farquhar, 2008 and references within). Merging the two treatments (+4°C and 4xCO_2), the higher evaporative demand balances the increased WUE and leads the model to simulate a soil moisture deficit. Note that using the SiB3 SWF leads to similar patterns (not shown) indicating that the strong environmental changes imposed here dominate the model's sensitivity to drought.

4. Discussion

4.1 Water stress functions

The parameterization of the drought-avoiding and tolerant strategies originally implemented in $ISBA_{CC}$ is not effective at simulating gas exchange fluxes when running the model over the Amazon forest, even when the soil moisture is not limiting. This conclusion is very likely to remain valid for other tropical forests, further studies need to assess their validity at global scale. Also, even if the original WSF were meant to represent isohydric and anisohydric drought responses, their performances are not consistent with physiological observations as there is little difference in modeled transpiration between both strategies due to a f_0 compensation effect. The linear WSF is more suitable for $ISBA_{CC}$ but, as the WSF is applied to g_m and not to g_s, the response to drought of g_s is not linear (Fig. 1). The SiB3 WSF responds too strongly to drought.

The difference in timing and amplitude of the vegetation response to drought when using the linear and SiB3 WSFs illustrate the model sensitivity to the chosen WSF. The WSF parameterization is also likely to be site dependent thus increasing the modelling challenge. The use of different WSF formulations in different land surface models (Egea et al., 2011; Zhou et al., 2013) reflects our inability to define the general behavior(s) for multi-species biomes in which the physiological processes are not yet fully understood. The use of 'hydrodynamic' models that do not include empirical soil moisture response functions, but instead predict drought-induced stomatal closure from the simulation of hydraulic potential, in the continuum soil-plant-atmosphere, has demonstrated some promising results (Williams et al., 2001; Fisher et al., 2006, 2007; Zeppel et al., 2008; McDowell et al., 2013).

4.2 Respiration

Despite measurement uncertainties, leaf respiration at Caxiuanã increases significantly with drought (Metcalfe et al., 2010), a process not captured by $ISBA_{CC}$. Other LSMs exhibit the same behavior as shown in a multi-model comparison against the TFE data (Powell et al., 2013). Although a decrease in leaf dark respiration is usually observed when photosynthetic capacity declines under drought, increases in leaf dark respiration have been observed elsewhere (Metcalfe et al., 2010; Atkin and

Macherel, 2009), including Amazonia during seasonal drought (Miranda et al., 2005). Powell et al., (2013) asks if we are missing a critical physiological process to accurately compute the plant carbon balance during drought. Even if changes in respiration might be smaller than the decrease in carbon assimilation when in drought (Atkin and Macherel, 2009), resolving this problem via further observations and research is vital considering the relevance of R_{ECO} to the net carbon flux.

4.3 Mortality

Mortality is a complex process, highly non linear in both time and space (Allen et al., 2010; Fisher et al., 2010; McDowell et al., 2011), and is represented by a wide array of algorithms in commonly used LSMs (McDowell et al., 2013). The inability to simulate drought-induced tree mortality is expected from a compartment carbon model such as $ISBA_{CC}$ that has no deterministic climate-mortality relationship. This is also a concern for LSMs linking mortality to negative carbon balance through the carbon starvation hypothesis (da Costa et al., 2010; Powell et al., 2013; McDowell et al., 2013). Also, $ISBA_{CC}$, like most LSMs, does not account for the water column pressure within the xylem, the drought induced cavitation process cannot be represented. Given recent evidence for drought-induced tree mortality (da Costa et al., 2010; Allen et al., 2010), the ability to simulate climate and drought-induced mortality in LSM is vital to assess the resilience of the Amazon forest under climate change and to estimate vegetation feedbacks. Besides, increased mortality risk during drought is associated with other processes like fire or insect outbreaks.

The detailed longitudinal datasets and the control over soil moisture that the throughfall exclusion experiments offer yield insights into ecological processes and dynamics are crucial for validating the processes represented by LSMs. At Caxiuanã baseline mortality rates in the experiment were strongly consistent with data from multiple nearby monitoring plot. In general, however, applying the results of these experiments to larger scale models will introduce uncertainty. For example, the observed decrease in biomass in the 1 ha throughfall exclusion plots was due to a few large trees that died first (Nepstad et al., 2007; Meir et al., 2009). Therefore, a combination of data sources seems the most effective way forward to constrain biomass and its sensitivity to climate within LSMs. For example data from long term inventory plots such as those from French Guyana since 1991, the RAINFOR datasets in Amazonia (Phillips et al., 2009) or trait-based mortality model outputs (e.g. Aubry-Kientz et al., 2013), should be used with the detailed results from the throughfall exclusion experiments.

4.4 Drought responses changes under different background conditions

Increases in CO_2 and temperature are modeled to have antagonistic effects on soil moisture through evapotranspiration because the WUE increases under higher CO_2 concentration (reducing transpiration) while higher temperature will enhance transpiration through a higher vapor pressure deficit. The simulated ET is highly reduced when imposing a high CO_2 concentration and $ISBA_{CC}$'s sensitivity to TFE is completely dampened. Unfortunately, there are no direct observations of the response to elevated CO_2 in tropical forests with which to constrain the reduced transpiration effect implemented in $ISBA_{CC}$ (and in other LSMs). There is some evidence for an recent increase in WUE due to CO_2-induced stomatal closure, both from fluxtowers (Keenan et al., 2013) and inferred from increasing global runoff (Gedney et al., 2006; Betts et al., 2007), but these results are disputed. Projections of the vegetation-climate interactions in the Amazon are highly sensitive to the response of the stomatal closure to a CO_2 enrichment (Cowling et al., 2008; Good et al., 2013). If, as recently suggested in Keenan et al., (2013), LSMs tend to underestimate CO_2-induced stomatal closure, it is likely that increasing WUE will partly offset future droughts and mitigate the expected drier and longer dry season (Fu et al., 2013). Therefore, the stomatal response, which regulates the water exchange within the soil-plant-atmosphere continuum, is fundamental to modelling the vegetation response to climate change (Berry et al., 2010). On the other hand, less ET reduces the water flux

towards the atmosphere, the local evaporative cooling, and might reduce precipitation through vegetation-atmosphere feedbacks. Numerous global climate model simulations of deforestation in the Amazon showed that regional precipitation is expected to decrease because of the combined influences of increased albedo, decreased surface roughness and decreased water recycling that accompany deforestation (e.g. Dickinson and Henderson-Sellers 1988; Malhi et al., 2008; Coe et al., 2009). Though increased WUE does not affect albedo or surface roughness like deforestation, it will affect the entire basin, not just the deforested areas.

5. Conclusions

Accurate representation of soil moisture and its seasonal dynamics is a prerequisite to simulate drought impacts on vegetation. Despite reasonable representation of the land surface hydrology, the land surface model $ISBA_{CC}$ fails to correctly simulate the vegetation response to the two Amazon rainfall exclusion experiments. First, a sensitivity analysis based on four WSFs showed that the amplitude and timing of $ISBA_{CC}$'s vegetation response to drought is quite sensitive to the chosen WSF. The drought-avoiding and tolerant strategies originally implemented in $ISBA_{CC}$ are not suitable for the Amazon forest on account of a g_s significantly lower than that observed. Of the functions we tested, the simplest linear function performs best.

While at Caxiuanã, the measured autotrophic respiration tends to be higher in the TFE than in the CTL plot, $ISBA_{CC}$ simulates an opposite trend. The observed loss of AGB, hiding the drought enhanced tree mortality, was greatly underestimated or even not captured by the model, as it doesn't represent mortality driven by strong climate anomalies. In the CTL plots, the representation of the vegetation (in terms of fluxes and stocks) is quite well simulated by $ISBA_{CC}$ but, physiological processes are missing to correctly estimate the vegetation response in case of drought, as most of LSMs (Powell et al., 2013). We also showed that the vegetation response to higher CO_2 and warmer temperature greatly affects its response to drought. As discussed and shown with other models, this can have great impacts to estimate the Amazon response to climate change and the vegetation feedbacks in climate projections.

Land surface models are designed to conduct investigations of processes with large spatial and temporal scales, and therefore, the vegetation representation necessarily includes many empirical approximations and coarse abstractions of reality. The definition of a generic drought response for Amazonian forests is evidently a difficult undertaking, particularly given evidence of the functional diversity of these forests in hydraulic functioning alone (Fisher et al., 2006; Baraloto et al. 2009). The introduction of more complex mechanistic models of drought stress removes the requirement to generate these empirical functions, but implies significantly higher model complexity and requirements for model specification using data that are difficult to acquire (root density, soil hydraulic conductivity, xylem conductance, etc.). The optimal strategy for drought simulation in land surface models remains unclear at this time. A better mechanistic understanding of the forest responses to drought under a warmer climate and higher CO_2 concentration is clearly needed, as some physiological processes are not yet fully understood and/or little observations are available, to improve LSMs.

References

Allen, C. D., Macalady, A., Chenchouni, H., Bachelet, D., McDowell, N., Vennetier, M., Gonzales, P., Hogg, T., Rigling, A., Breshears, D., Hogg, E. H. (Ted), Gonzalez, P., Fenshaml, R., Zhangm, Z., Castro, J., Demidovao, N., Limp, J. H., Allard, G., Runningr, S. W., Semerci, A., Cobbt, N.: Climate-induced forest mortality: a global overview of emerging risks, Forest Ecol. Manag., 259,

660–684, doi:10.1016/j.foreco.2009.09.001, 2010.

Anderson, L. O., Malhi, Y., Aragao, L. E. O. C., Ladle, R., Arai, E., Barbier, N., and Phillips, O.: Remote sensing detection of droughts in Amazonian forest canopies, The New Phytol., 187, 733–750, doi:10.1111/j.1469-8137.2010.03355.x, 2010.

Atkin, O. K. and Macherel, D.: The crucial role of plant mitochondria in orchestrating drought tolerance, Ann. Bot.-London, 103, 581–597, 2009.

Aubry-Kientz, M., Hérault, B., Ayotte-Trépanier, C., Baraloto, C., and Rossi, V.: Toward trait-based mortality models for tropical forests, PloS One, 8, e63678, doi:10.1371/journal.pone.0063678, 2013.

Baker, I. T., Prihodko, L., Denning, A. S., Goulden, M. L., Miller, S., and da Rocha, H. R.:Seasonal drought stress in the amazon: reconciling models and observations, J. Geophys. Res., 113, 2005–2012, doi:10.1029/2007JG000644, 2008.

Baraloto, C., Timothy Paine, C. E., Patino, S., Bonal, D., Herault, B., and Chave, J.: Functional trait variation and sampling strategies in species-rich plant communities, Funct. Ecol., 24, 208–216, 2009.

Beer, C., Reichstein, M., Tomelleri, E., Ciais, P., Jung, M., Carvalhais, N., Rodenbeck, C., Arain, M. A., Baldocchi, D., Bonan, G. B., Bondeau, A., Cescatti, A., Lasslop, G., Anders, L., Lomas, M., Luyssaert, S., Margolis, H., Olewson, K. W., Roupsard, O., Veenendaal, E., Viovy, N., Williams, C., Woodward, F. I., and Papale, D.: Terrestrial gross carbon dioxide uptake: global distribution and covariation with climate, Science, 329, 834–838, doi:10.1126/science.1184984, 2010.

Berry, J. A., Beerling, D. J., and Franks, P. J.: Stomata: key players in the earth system, past and present, Curr. Opin. Plant Biol., 13, 233–240, doi:10.1016/j.pbi.2010.04.013, 2010.

Betts, R. A., Boucher, O., Collins, M., Cox, P. M., Fallon, P. D., Gedney, N., Hemming, D. L., Huntingford, C., Jones, C., Sexton, D. M. H., and Webb, M. J.: Projected increase in continental runoff due to plant responses to increasing carbon dioxide, Nature, 448, 1037–1041, doi:10.1038/nature06045, 2007.

Booth, B. B. B., Jones, C., Collins, M., Totterdell, I. J., Cox, P. M., Sitch, S., Huntingford, C., Betts, R. A., Harris, G. R., and Lloyd, J.: High sensitivity of future global warming to land carbon cycle processes, Environ. Res. Lett., 7, 1–8, doi:10.1088/1748-9326/7/2/024002, 2012.

Brando, P. M., Nepstad, D. C., Davidson, E. A, Trumbore, S. E., Ray, D., Camargo, P.: Drought effects on litterfall, wood production, and belowground carbon cycling in an Amazon forest: results of a throughfall reduction experiment, Philosophical Transactions of the Royal Society of London – Biological Sciences, 363, 1839–1848, 2008.

Calvet, J. C., Noilhan, J., Roujean, J. L., Bessemoulin, P., Cabelguenne, M., Olioso, A., and Wigneron, J. P.: An interactive vegetation SVAT model tested against data from six contrasting sites, Agr. Forest Meteorol., 92, 73–95, 1998.

Calvet, J. C., Rivalland, V., Picon-Cochard, C., and Guehl, J. M.: Modelling forest transpiration and CO2 fluxes response to soil moisture stress, Agr. Forest Meteorol., 124, 143–156, 2004.

Carrer, D., Roujean, J. L., Lafont, S., Calvet, J. C., Boone, A., Decharme, B., Delire, C., and

Gastellu-Etchegorry, J. P.: A canopy radiative transfer scheme with explicit FAPAR for the interactive vegetation model ISBA-A-gs: impact on carbon fluxes, J. Geophys. Res.-Biogeo., 118, 1–16, doi:10.1002/jgrg.20070, 2013.

Chen, B., Black, T. A., Coops, N. C., Hilker, T., Trofymow, J. A. T., and Morgenstern, K.: Assessing Tower Flux Footprint Climatology and Scaling Between Remotely Sensed and Eddy Covariance Measurements, Bound.-Lay. Meteorol., 130, 137–167, 2008.

Coe, M. T., Costa, M. H., and Soares-Filho, B. S.: The influence of historical and potential future deforestation on the stream flow of the Amazon River – land surface processes and atmospheric feedbacks, J. Hydrol., 369, 165–174, doi:10.1016/j.jhydrol.2009.02.043, 2009.

da Costa, A. C. L., Galbraith, D., Almeida, S., Portela, B. T. T., da Costa, M., de Athaydes Silva Junior, J., Braga, A. P., de Gonçalves, P. H. L., de Oliveira, A. A. R., Fisher, R., Phillips, O. L., Metcalfe, D. B., Levy, P., and Meir, P.: Effect of 7 yr of experimental drought on the aboveground biomass storage of an eastern Amazonian rainforest, New Phytol., 187, 579–591, 2010.

Cowling, S. A., Shin, Y., Pinto, E., and Jones, C. D.: Water recycling by Amazonian vegetation: coupled versus uncoupled vegetation–climate interactions, Phil. Trans. R. Soc. B, 363, 1865–1871, 2008.

Cox, P. M., Betts, R. A., Jones, C. D., Spall, S. A., and Totterdell, I. J.: Acceleration of global warming due to carbon-cycle feedbacks in a coupled climate model, Nature, 408, 184–187, 2000.

Cox, P. M., Betts, R. A., Collins, M., Harris, P. P., Huntingford, C., and Jones, C. D.: Amazonian forest dieback under climate-carbon cycle projections for the 21st century, Theor. Appl. Climatol., 78, 137–156, 2004.

Davidson, E. A., Nepstad, D. C., Ishida, F. Y., Brando, P. M.: Effects of an experimental drought and recovery on soil emissions of carbon dioxide, methane, nitrous oxide, and nitric oxide in a moist tropical forest, Global Change Biology, 14, 2582–2590, 2008

Decharme, B., Douville, H., Boone, A., Habets, F., and Noilhan, J.: Impact of an exponential profile of saturated hydraulic conductivity within the ISBA LSM: simulations over the Rhone basin, J. Hydrometeorol., 7, 61–80, 2006.

Decharme, B., Boone, A., Delire, C., and Noihlan, J.: Local evaluation of the Interaction between Soil Biosphere Atmosphere soil multilayer diffusion scheme using four pedotransfer functions, J. Geophys. Res., 116, 1984–2012, 2011.

Decharme, B., Martin, E., and Faroux, S.: Reconciling soil thermal and hydrological lower boundary conditions in land surface models, J. Geophys. Res.-Atmos., 118, 1–16, 2013.

Dickinson, R. E. and Henderson Sellers, A.: Modelling tropical deforestation: a study of GCM land surface parametrizations, Q. J. Roy. Meteor. Soc., 114, 439–462, 1988.

Domingues, T. F., Martinelli, L. A., and Ehleringer, J. R.: Ecophysiological traits of plant functional groups in forest and pasture ecosystems from eastern Amazonia, Brazil, Plant Ecol., 193, 101–112, 2007.

Douville, H., Ribes, A., Decharme, B., Alkama, R., and Sheffield, J.: Anthropogenic influence on multidecadal changes in reconstructed global evapotranspiration, Nature Climate Change, 3,59–62,

2013.

Egea, G., Verhoef, A., and Vidale, P. L.: Towards an improved and more flexible representation of water stress in coupled photosynthesis–stomatal conductance models, Agr. Forest Meteorol., 151, 1370–1384, 2011.

Eltahir, E. and Bras, R. L.: Precipitation recycling in the Amazon Basin, Q. J. Roy. Meteor. Soc., 120, 861–880, 1994.

Fisher, R. A., Williams, M., Do Vale, R. L., Da Costa, A. L., and Meir, P.: Evidence from Amazonian forest is consistent with isohydric control of leaf water potential, Plant Cell Environ., 29, 151–165, 2006.

Fisher, R. A., Williams, M., da Costa, A. L., Malhi, Y., da Costa, R. F., Almeida, S., and Meir, P.: The response of an Eastern Amazonian rain forest to drought stress: results and modelling analyses from a throughfall exclusion experiment, Glob. Change Biol., 13, 2361–2378, 2007.

Fisher, R. A., McDowell, N., Purves, D., Moorcroft, P., Sitch, S., Cox, P., Huntingford, C., Meir, P., and Woodward, F. I.: Assessing uncertainties in a second-generation dynamic vegetation model due to ecological scale limitations, New Phytol., 187, 666–681, 2010.

Friedlingstein, P., Cox, P., Betts, R., Bopp, L., von Bloh, W., Brovkin, V., Cadule, P., Doney, S., Eby, M., Fung, I., Bala, G., John, J., Jones, C., Joos, F., Kato, T., Kawamiya, M., Knorr, W., Lindsay, K., Matthews, H. D., Raddatz, T., Rayner, P., Reick, C., Roeckner, E., Schnitzler, K. G., Schnur, R., Strassmann, K.,Weaver, A. J., Yoshikawa, C., and Zeng, N.: Climatecarbon cycle feedback analysis: results from the C4MIP model intercomparison, J. Climate, 19, 3337–3353, 2006.

Fu, R., Yin, L., Li, W., Arias, P. A., Dickinson, R. E., Huang, L., Chakraborty, S., Fernandes, K., Liebmann, B., Fisher, R. A., and Myneni, R. B.: Increased dry-season length over southern Amazonia in recent decades and its implication for future climate projection, P. Natl. Acad. Sci. USA, 110, 18110–18115, doi:10.1073/pnas.1302584110, 2013.

Galbraith, D., Levy, P. E., Sitch, S., Huntingford, C., Cox, P., Williams, M., and Meir, P.: Multiple mechanisms of Amazonian forest biomass losses in three dynamic global vegetation models under climate change, New Phytol., 187, 647–665, 2010.

Gatti, L. V., Gloor, M., Miller, J. B., Doughty, C. E., Malhi, Y., Domingues, L. G., Basso, L. S., Martinewski, A., Correia, C. S. C., and Borges, V. F.: Drought sensitivity of Amazonian carbon balance revealed by atmospheric measurements, Nature, 506, 76–80, 2014.

Gedney, N., Cox, P. M., Betts, R. A., Boucher, O., Huntingford, C., and Stott, P. A.: Detection of a direct carbon dioxide effect in continental river runoff records, Nature, 439, 835–838, 2006.

Gibelin, A. L., Calvet, J. C., Roujean, J. L., Jarlan, L., and Los, S. O.: Ability of the land surface model ISBA-A-gs to simulate leaf area index at the global scale: comparison with satellites products, J. Geophys. Res., 111, 1984–2012, 2006.

Gibelin, A. L., Calvet, J. C., and Viovy, N.: Modelling energy and CO2 fluxes with an interactive vegetation, land surface model, Evaluation at high and middle latitudes, Agr. Forest Meteorol., 148, 1611–1628, 2008.

Good, P., Jones, C., Lowe, J., Betts, R., and Gedney, N.: Comparing tropical forest projections from two generations of Hadley Centre Earth System models, HadGEM2-ES and HadCM3LC, J. Climate, 26, 495–511, 2013.

Guimberteau, M., Ducharne, A., Ciais, P., Boisier, J. P., Peng, S., De Weirdt, M., and Verbeeck, H.: Testing conceptual and physically based soil hydrology schemes against observations for the Amazon Basin, Geosci. Model Dev., 7, 1115–1136, doi:10.5194/gmd-7-1115-2014, 2014.

Huntingford, C., Zelazowski, P., Galbraith, D., Mercado, L. M., Sitch, S., Fisher, R. A., Lomas, M., Walker, A. P., Jones, C. D., Booth, B. B. B., Malhi, Y., Hemming, D., Kay, G., Good, P., Lewis, S.L., Phillips, O. L., Atkin, O. K., Lloyd, J., Gloor, E., Zaragoza-Castells, J., Meir, P., Betts, R., Harris, P. P, Nobre, C., Marengo, C., and Cox, P. M.: Simulated resilience of tropical rainforests to CO2-induced climate change, Nat. Geosci., 6, 268–273, 2013.

Jacobs, C. M. J.: Direct impact of atmospheric CO2 enrichment on regional transpiration, Ph.D. thesis, Agricultural University, Wageningen, 1994.

Joetzjer, E., Douville, H., Delire, C., and Ciais, P.: Present-day and future Amazonian precipitation in global climate models: CMIP5 versus CMIP3, Clim. Dynam., 41, 2921–2936, 2013.

Jupp, T. E., Cox, P. M., Rammig, A., Thonicke, K., Lucht, W., and Cramer, W.: Development of probability density functions for future South American rainfall, New Phytol., 187, 682–693, 2010.

Keenan, T. F., Hollinger, D. Y., Bohrer, G., Dragoni, D., Munger, J. W., Schmid, H. P., and Richardson, A. D.: Increase in forest water-use efficiency as atmospheric carbon dioxide concentrations rise, Nature, 499, 324–327, doi:10.1038/nature12291, 2013.

Lewis, S. L., Brando, P. M., Phillips, O. L., van der Heijden, G. M., and Nepstad, D.: The 2010 Amazon drought, Science, 331, 554–554, doi:10.1126/science.1200807, 2011.

Lloyd, J. and Farquhar, G. D.: Effects of rising temperatures and [CO2] on the physiology of tropical forest trees, Philos. T. R. Soc. B, 363, 1811–1817, 2008.

Malhi, Y., Wood, D., Baker, T. R., Wright, J., Phillips, O. L., Cochrane, T., Meir, P., Chave, J., Almeida, S., Arroyo, L., Higuchi, N., Killeen, T. J., Laurance, S. G., Laurance, W. F., Lewis, S. L., Monteagudo, A., Neill, D. A., Núñez Vargas, P., Pitman, N. C. A., Quesada, C. A., Salomão, R., Silva, J. N. M., Torres Lezama, A., Terborgh, J., Vásquez Martínez, R., and Vinceti, B.: The regional variation of aboveground live biomass in old-growth Amazonian forests, Glob. Change Biol., 12, 1107–1138, 2006.

Malhi, Y., Roberts, J. T., Betts, R. A., Killeen, T. J., Li, W., and Nobre, C. A.: Climate change, deforestation, and the fate of the Amazon, Science, 319, 169–172, 2008.

Malhi, Y., Aragao, L. E. O., Metcalfe, D. B., Paiva, R., Quesada, C. A., Almeida, S., Anderson, L., Brando, P., Chamber, J. Q., and da Costa, A. C. L.: Comprehensive assessment of carbon productivity, allocation and storage in three Amazonian forests, Glob. Change Biol., 15, 1255–1274, 2009.

Markewitz, D., Devine, S., Davidson, E. A., Brando, P., and Nepstad, D. C.: Soil moisture depletion under simulated drought in the Amazon: impacts on deep root uptake, New Phytol., 187, 592–607, 2010.

McDowell, N. G., Beerling, D. J., Breshears, D. D., Fisher, R. A., Raffa, K. F., and Stitt, M.: The interdependence of mechanisms underlying climate-driven vegetation mortality, Trends Ecol. Evol., 26, 523–532, 2011.

McDowell, N. G., Fisher, R. A., Xu, C., Domec, J. C., Holtta, T., Mackay, S., Sperry, J. S., Boutz, A., Dickman, L., and Gehres, N.: Evaluating theories of drought-induced vegetation mortality using a multimodel–experiment framework, New Phytol., 200, 304–321, 2013.

Meir, P., Cox, P., and Grace, J.: The influence of terrestrial ecosystems on climate, Trends Ecol. Evol., 21, 254–260, 2006.

Meir, P., Brando, P. M., Nepstad, D., Vasconcelos, S., Costa, A. C. L., Davidson, E., Almeida, S., Fisher, R. A., Sotta, E. D., and Zarin, D.: The effects of drought on Amazonian rain forests, in: Amazonia and global change, edited by: Keller, M., Bustamante, M., Gash, J., and Silva Dias, P., Geoph. Monog. Series, 186, 429–449, 2009.

Metcalfe, D. B., Meir, P., Aragao, L. E. O. C., Lobo-do-Vale, R., Galbraith, D., Fisher, R. A., Chaves, M. M., Maroco, J. P., da Costa, A. C. L., de Almeida, S. S., Braga, A. P., Gonçalves, P. H. L, de Athaydes, J., da Costa, M., Portela, T. T. B., de Oliveira, A. A. R., Malhi, and Williams, M.: Shifts in plant respiration and carbon use efficiency at a large-scale drought experiment in the eastern Amazon, New Phytol., 187, 608–621, 2010.

Miranda, E. J., Vourlitis, G. L., Filho, N. P., Priante, P. C., Campelo, J. H., Suli, G. S., Fritzen, C. L., De Almeida Lobo, F., and Shiraiwa, S.: Seasonal variation in the leaf gas exchange of tropical forest trees in the rain forest–savanna transition of the southern Amazon basin, J. Trop. Ecol., 21, 451–460, 2005.

van der Molen, M. K., Dolman, A. J., Ciais, P., Eglin, T., Gobron, N., Law, B. E., Meir, P., Peters, W., Phillips, O. L., Reichstein, M., Chen, T., Dekker, S. C., Doubková, M., Friedl, M. A., Jung, M., van den Hurk, B. J. J. M., de Jeu, R. A. M., Kruijt, B., Ohta, T., Rebel, K. T., Plummer, S., Seneviratne, S. I., Sitch, S., Teuling, A. J., van der Werf, G. R., and Wang, G.: Drought and ecosystem carbon cycling, Agr. Forest Meteorol., 151, 765–773, 2011.

Nepstad, D. C., Moutinho, P., Dias, M. B., Davidson, E., Cardinot, G., Markewitz, D., Figueiredo, R., Vianna, N., Chambers, J., Ray, D., Guerreiros, J. B., Lefebvre, P., Sternberg, L., Moreira, M., Barros, L., Ishida, F. Y., Tohlver, I., Belk, E., Kalif, K., and Schwalbe, K.: The effects of partial throughfall exclusion on canopy processes, aboveground production and biogeochemistry of an Amazon forest, J. Geophys. Res.-Atmos., 107, 1–18, 2002.

Nepstad, D. C., Lefebvre, P., Lopes da Silva, U., Tomasella, J., Schlesinger, P., Solorzano, L., Moutinho, P., Ray, D., and Guerreira Benito, J.: Amazon drought and its implications for forest flammability and tree growth: a basin-wide analysis, Glob. Change Biol., 10, 704–717, 2004.

Nepstad, D. C., Tohver, I. M., Ray, D., Moutinho, P., and Cardinot, G.: Mortality of large trees and lianas following experimental drought in an Amazon forest, Ecology, 88, 2259–2269, 2007.

Noilhan, J., and Planton, S. : A simple parameterization of land surface processes for meteorological models, Mon. Weather Rev., 117, 536– 549, 1989.

Noilhan, J. and Mahfouf, J.-F.: The ISBA land surface parameterisation scheme, Global Planet Change, 13, 145–159, 1996.

Pan, Y., Birdsey, R. A., Fang, J., Houghton, R., Kauppi, P. E., Kurz, W. A., Phillips, O. L., Shvidenko, A., Lewis, S. L., Canadell, J. G., Ciais, P., Jackson, R. B., Pacala, S. W., McGuire, A. D., Piao, S., Rautiainen, A., Sitch, S., and Hayes, D.: A large and persistent carbon sink in the world's forests, Science, 333, 988–993, 2011.

Phillips, O. L., Aragao, L. E. O. C., Lewis, S. L., Fisher, J. B., Lloyd, J., Lopez-Gonzalez, G., Malhi, Y., Monteagudo, A., Peacock, J., Quesada, C. A., van der Heijden, G., Almeida, S.,Amaral, I., Arroyo, L., Aymard, G., Baker, T. R., Banki, O., Blanc, L., Bonal, D., Brando, P., Chave, J., Alves de Oliveira, A. C., Cardozo, N. D., Czimczik, C. I., Feldpausch, T. R., Freitas, M. A., Gloor, E., Higuchi, N., Jimenez, E., Lloyd, G., Meir, P., Mendoza, C., Morel, A., Neill, D. A., Nepstad, D., Patino, S., Cristina Penuela, M., Prieto, A., Ramirez, F., Schwarz, M., Silva, J., Silveira, M., Thomas, A. S., ter Steege, H., Stropp, J., Vasquez, R., Zelazowski, P., Alvarez Davila, E., Andelman, S., Andrade, A., Chao, K.-J., Erwin, T., Di Fiore, A., Honorio C, E., Keeling, H., Killeen, T. J., Laurance,W. F., Pena Cruz, A., Pitman, N. C. A., Nunez Vargas, P., Ramirez-Angulo, H., Rudas, A., Salamao, R., Silva, N., Terborgh, J., and Torres-Lezama, A.: Drought sensitivity of the Amazon rainforest, Science, 323, 1344–1347, 2009.

Phillips, O. L., Van Der Heijden, G., Lewis, S. L., Lopez-Gonzalez, G., Aragao, L. E. O. C., Lloyd, J., Malhi, Y., Monteagudo, A., Almeida, S., Davila, E. A., Amaral, I., Andelman, S., Andrade, A., Arroyo, L., Aymard, G., Baker, T. R., Blanc, L., Bonal, D., De Oliveira, A. C. A., Chao, K.-J., Cardozo, N. D., Da Costa, L., Feldpausch, T. R., Fisher, J. B., Fyllas, N. M., Freitas, M. A., Galbraith, D., Gloor, E., Higuchi, N., Honorio, E., Jimenez, E., Keeling, H., Killeen, T. J., Lovett, J. C., Meir, P., Mendoza, C., Morel, A., Vargas, P. N., Patino, S., Peh, K. S. H., Cruz, A. P., Prieto, A., Quesada, C. A., Ramirez, F., Ramirez, H., Rudas, A., Salamao, R., Schwarz, M., Silva, J., Silveira, M., Ferry Slik, J. W., Sonke, B., Thomas, A. S., Stropp, J., Taplin, J. R. D., Vasquez, R., Vilanova, E.: Drought–mortality relationships for tropical forests, New Phytol., 187, 631–646, 2010.

Picon, C., Guehl, J. M., and Ferhi, A.: Leaf gas exchange and carbon isotope composition responses to drought in a drought – avoiding (Pinus pinaster) and a drought-tolerant (Quercus petraea) species under present and elevated atmospheric CO2 concentrations, Plant Cell Environ., 19, 182–190, 1996.

Potter, C. S. and Klooster, S. A.: Detecting a terrestrial biosphere sink for carbon dioxide: interannual ecosystem modeling for the mid 1980s, Climatic Change, 42, 489–503, 1999.

Poulter, B., Heyder, U., and Cramer, W.: Modeling the sensitivity of the seasonal cycle of GPP to dynamic LAI and soil depths in tropical rainforests, Ecosystems, 12, 517–533, 2009.

Powell, T. L., Galbraith, D. R., Christoffersen, B. O., Harper, A., Imbuzeiro, H. M. A., Rowland, L., Almeida, S., Brando, P. M., da Costa, A. C. L., Costa, M. H., Levine, N. M., Malhi, Y., Saleska, S. R., Sotta, E., Williams, M., Meir, P., and Moorcroft, P.: Confronting model predictions of carbon fluxes with measurements of Amazon forests subjected to experimental drought, New Phytol., 200, 350–365, 2013.

Rammig, A., Jupp, T., Thonicke, K., Tietjen, B., Heinke, J., Ostberg, S., Lucht, W., Cramer, W., and Cox, P.: Estimating the risk of Amazonian forest dieback, New Phytol., 187, 694–706, 2010.

Reichstein, M., Bahn, M., Ciais, P., Frank, D., Mahecha, M. D., Seneviratne, S. I., Zscheischler, J., Beer, C., Buchmann, N., Frank, D. C., Papale, D., Rammig, A., Smith, P., Thonicke, K., van der Velde, M., Vicca, S.,Walz, A., andWattenbach, M.: Climate extremes and the carbon cycle, Nature, 500, 287–295, 2013.

Ruivo, M. L. P. and Cunha, E. S.: Mineral and organic components in archaeological black earth and yellow latosol in Caxiuanã, Amazon, Brazil, Adv. Ecol. Sci., 18, 1113–1121, 2003.

Sakaguchi, K., Zeng, X., Christoffersen, B. J., Restrepo-Coupe, N., Saleska, S. R., and Brando, P. M.: Natural and drought scenarios in an east central Amazon forest: fidelity of the Community Land Model 3.5 with three biogeochemical models, J. Geophys. Res., 116, G01029, doi:10.1029/2010JG001477, 2011.

Shiogama, H., Emori, S., Hanasaki, N., Abe, M., Masutomi, Y., and Takahashi, K.: Observational constraints indicate risk of drying in the Amazon basin, Nature Communications, 3, 10 253–257, doi:10.1038/ncomms1252, 2011.

Williams, M., Bond, B. J., and Ryan, M. G.: Evaluating different soil and plant hydraulic constraints on tree function using a model and sap flow data from ponderosa pine, Plant Cell Environ., 24, 679–690, 2001.

Woodward, F. I.: Climate and Plant Distribution, Cambridge University Press, 1987.

Zeppel, M., Macinnis-Ng, C., Palmer, A., Taylor, D., Whitley, R., Fuentes, S., Yunusa, I., Williams, M., and Eamus, D.: An analysis of the sensitivity of sap flux to soil and plant variables assessed for an Australian woodland using SPA, Funct. Plant Biol., 35, 509–520, 2008.

Zhou, S., Duursma, R., Medlyn, B. E., Kelley, J.W. G., and Prentice, I. C.: How should we model plant responses to drought? An analysis of stomatal and non-stomatal responses to water stress, Agr. Forest Meteorol., 182–183,204–214, 2013.

Acknowledgments

The authors are grateful to Colin Prentice, Jerôme Chave, Simon Donner, Bruno Hérault, David Galbraith, Paulo Brando and Daniel Markewitz for helpful discussions and/or for providing datasets. P.M. acknowledges support from ARC FT FT110100457 and NERC NE/J011002/1. Thanks are also due to the AMAZALERT FP7 project for supporting this study.

Predicting the response of the Amazon rainforest to persistent drought conditions under current and future climates : a major challenge for global land surface models

Tables and Figures

TABLE 1 – $ISBA_{CC}$: Notation and main equations for the photosynthesis model

Symbols	Units	Definition
A_m	$kg_{CO2}.m^{-2}.s^{-1}$	Photosynthesis rate (light saturated)
C_a	$ppmv$	Atmospheric CO_2 concentration
C_i	$ppmv$	Leaf internal CO_2 concentration
D_s	$g.kg^{-1}$	Saturation deficit at the leaf surface
D_{max}	$g.kg^{-1}$	Saturation deficit inducing stomatal closure
f	unitless	coupling factor
f_0	unitless	coupling factor at saturating air humidity ($D_s = 0$)
f_0^*	unitless	coupling factor in well-watered conditions and at saturating air humidity ($D_s = 0$)
f_{min}	unitless	coupling factor at maximum air humidity deficit ($D_s = D_{max}$)
Γ	$ppmv$	CO_2 concentration compensation point
g_m	$mm.s^{-1}$	Mesophyll conductance defined as the light saturated rate of photosynthesis (Jacobs, 1994)
g_m^*	$mm.s^{-1}$	g_m in well-watered conditions
g_s	$mm.s^{-1}$	Stomatal conductance

Equations

$$g_m = \frac{A_m}{C_i - \Gamma} \text{ ; at high light intensity and low Ci} \qquad \textbf{[Eq.1]}$$

$$f = \frac{C_i - \Gamma}{C_a - \Gamma} \qquad \textbf{[Eq.2]}$$

$$f = f_0 \cdot (1 - \frac{D_s}{D_{max}}) + f_{min} \cdot \frac{D_s}{D_{max}} \qquad \textbf{[Eq.3]}$$

TABLE 2 – **Description of $ISBA_{CC}$: Water Stress Functions.**

Name	**Soil Wetness Index**	**Water Stress functions applied to g_m**	**Water Stress functions applied to f_0**
Avoiding	$SWI \geq 1$	$ln(g_m^*) = 4.7 - 7.f_0^*$	
	$SWIc < SWI < 1$	$g_m = g_m^*$	$f_0 = f_0^* - (f_0^* - f_0^N) \cdot \frac{(1-SWI)}{(1-SWIc)}$
	$SWI \leq SWIc$	$g_m = g_m^* \cdot \frac{SWI}{SWIc}$	$f_0 = \frac{2.8 - ln(g_m)}{7}$
Tolerant	$SWI \geq 1$	$ln(g_m^*) = 4.7 - 7.f_0^*$	
	$SWIc < SWI < 1$	$g_m = g_m^* - (g_m^* - g_m^N) \cdot \frac{(1-SWI)}{(1-SWIc)}$	$f_0 = f_0^*$
	$SWI \leq SWIc$	$g_m = g_m^N \cdot \frac{SWI}{SWIc}$	$f_0 = \frac{2.8 - ln(g_m)}{7}$
Linear		$g_m = SWI \cdot g_m^*$	$f_0 = 0.74$
SiB3		$g_m = \frac{(1+\alpha) \cdot SWI}{(\alpha \cdot SWI)} \cdot g_m^*$; $\alpha = 0.1$	$f_0 = 0.74$

Symbol	**Description**	
SWI	Soil Wetness index	$SWI = \frac{\Theta - \Theta_{wilt}}{\Theta - \Theta_{fc}}$
Θ	Soil water content ($m^3.m^{-3}$)	
Θ_{fc}	Field capacity ($m^3.m^{-3}$	
Θ_{wilt}	Wilting point ($m^3.m^{-3}$	
SWI_c	Critical extractable Soil Wetness Index (drought-avoiding and tolerant)	$SWI_c = 0.3$
f_0^N	Minimum value of f_0 at $SWI = SWI_c$ (drought-avoiding)	$f_0^N = \frac{ln(g_m^*) - 2.8}{7}$
g_m^N	Value of g_m at $SWI = SWI_c$ in $mm.s^{-1}$ (drought-tolerant)	$ln(g_m^N) = 2.8 - 7.f_0^*$

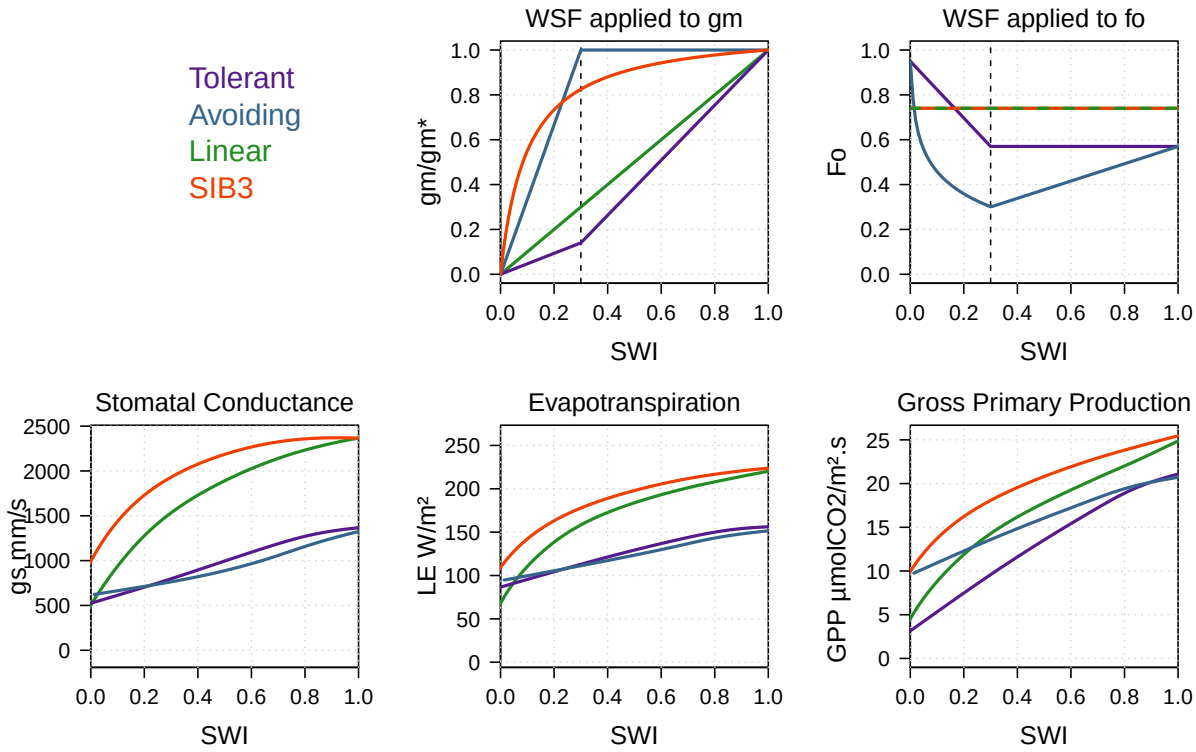

FIGURE 1 – *Graphical representation the mesophyll conductance (gm),the coupling factor at saturating air humidity (f_0), the stomatal conductance (gs), the evapotranspiration (LE) and the Gross Primary Production (GPP) for the four Water Stress Functions (WSF) used in this study against the Soil Wetness Index (SWI).*

TABLE 3 – References and available period for observations used in this study.

Variables	Symbol	Units	Tapajós	Caxiuanã
Soil Water Content	SWC	$m^3.m^{-3}$	1999-2005 Brando et al. 2008 Markewitz et al. 2010	2001-2004 Fisher et al. 2007
Stomatal Conductance	gs	$mmol_{CO_2}.m^{-2}.s^{-1}$		2002-2003 Fisher et al. 2006
Evapotranspiration	ET	$mm.day^{-1}$	1999-2004 (modeled) Markewitz et al. 2010	
Gross Primary Production	GPP	$\mu mol_{CO_2}.m^{-2}.s^{-1}$		2002-2003 (modeled) Fisher et al. 2007
Ecosystem Respiration	R_e	$t_C.ha^{-1}.yr^{-1}$		2001-2005 Metcalfe et al. 2010
Autotrophic Respiration	R_a	$t_C.ha^{-1}.yr^{-1}$		2001-2005 Metcalfe et al. 2010
Leaf Respiration	R_l	$t_C.ha^{-1}.yr^{-1}$		2001-2005 Metcalfe et al. 2010
Wood Respiration	R_w	$t_C.ha^{-1}.yr^{-1}$		2001-2005 Metcalfe et al. 2010
Root Respiration	R_r	$t_C.ha^{-1}.yr^{-1}$		2001-2005 Metcalfe et al. 2010
Soil Respiration	R_s	$t_C.ha^{-1}.yr^{-1}$	1999 - 2004 Davidson et al. 2008	2001-2005 Metcalfe et al. 2010
Leaf Area Index	LAI	$m^2.m^{-2}$	2000-2005 Brando et al. 2008	2001-2007 Fisher et al. 2007
Above Ground Biomasse	AGB	$t_C.ha^{-1}.yr^{-1}$	1999-2005 Brando et al. 2008	2000-2008 da Costa et al. 2010

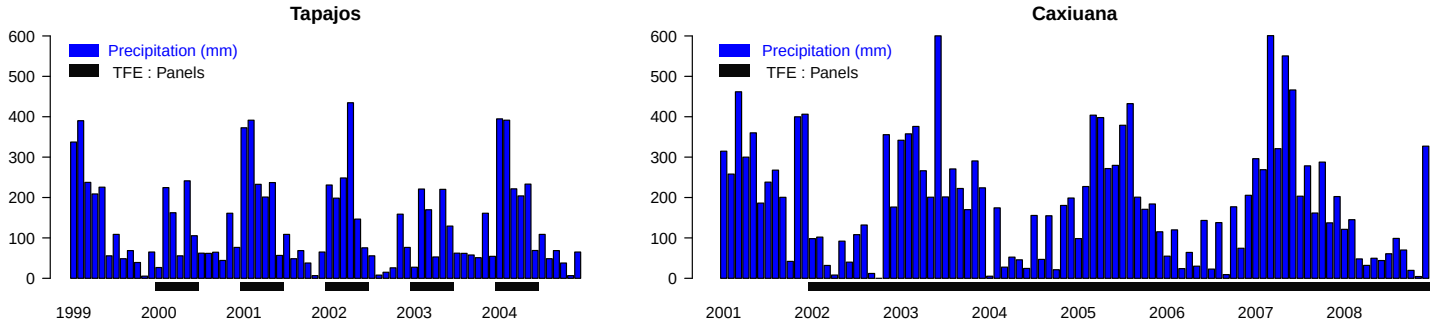

FIGURE 2 – *Monthly observed precipitation at Tapajós and Caxiuanã. Horizontal black bars indicate when panels were applied for the TFE experiments.*

TABLE 4 – Summary of ISBA$_{CC}$ simulations

Meteorological forcing	**WSF Tolerant**	**WSF Avoiding**	**WSF Linear**	**WSF SiB3**	**sites**
in situ	X	X	X	X	Caxiuanã & Tapajós
in situ $+4^0C$			X	X	Caxiuanã
in situ x4$[CO_2]$			X	X	Caxiuanã
in situ $+4^0C$ x4$[CO_2]$			X	X	Caxiuanã

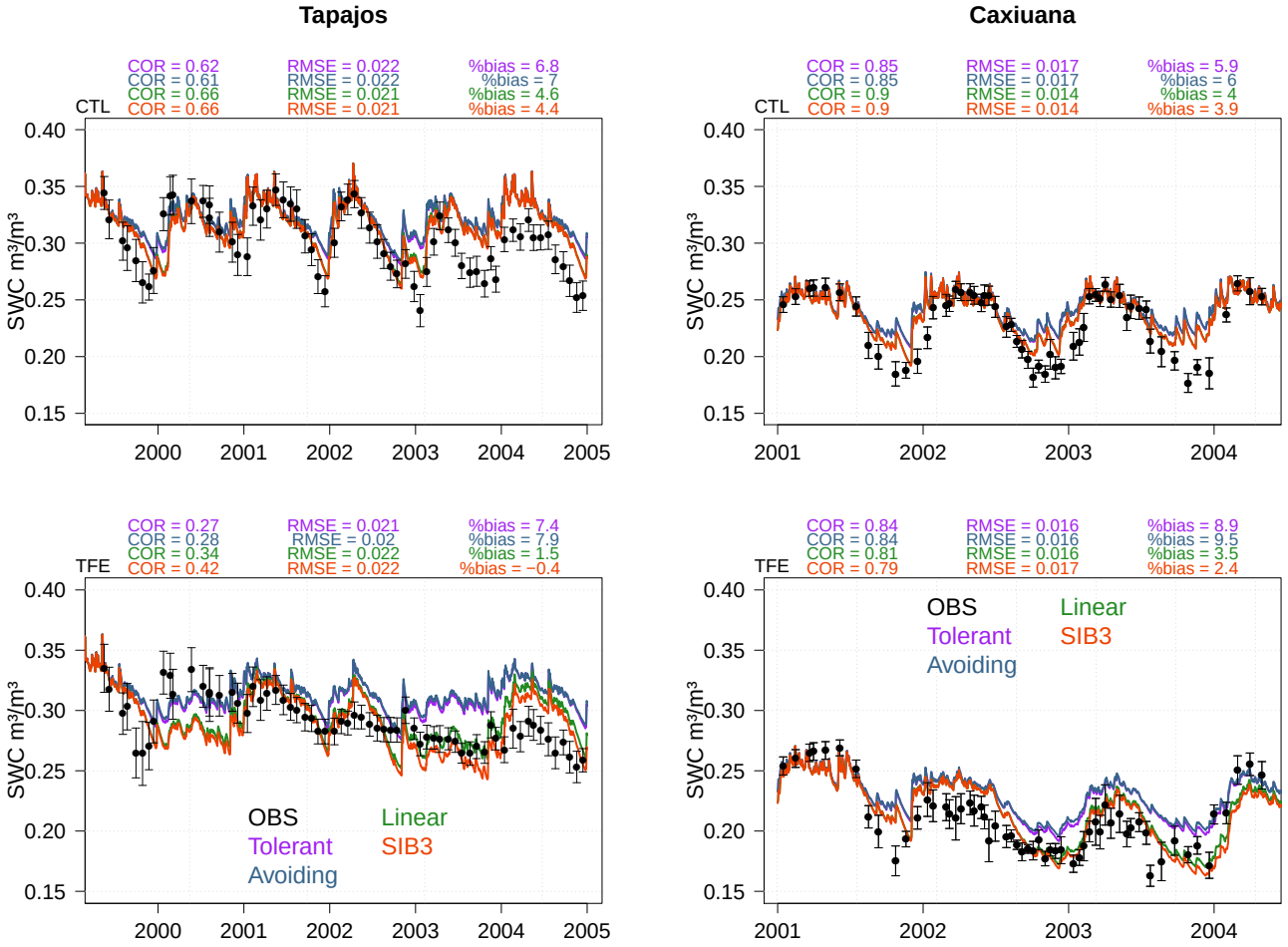

FIGURE 3 – *Daily observed and simulated Soil Water Content with the 4 WSF at Tapajós (left) and Caxiuanã (right) for both CTL (top) and TFE (bottom) plots. The SWC measured at the TFE plots were rescaled to have identical SWC than the CTL plots during the baseline year.*

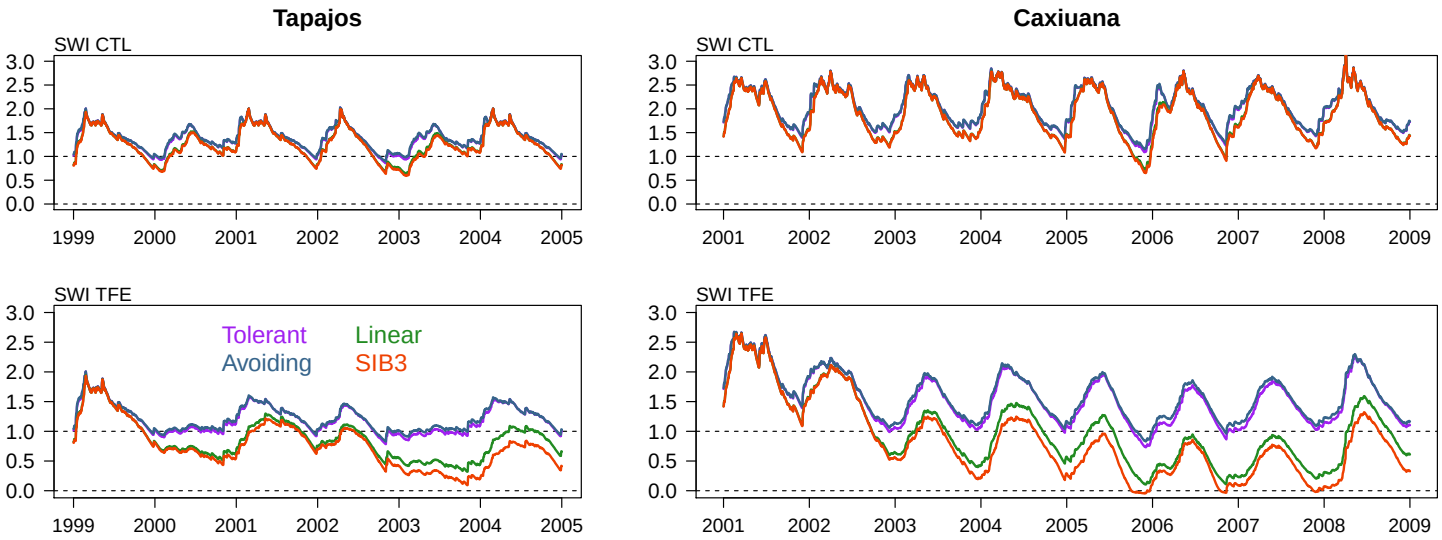

FIGURE 4 – *Simulated daily Soil Wetness Index (SWI) with the 4 WSF at Tapajós (left) and Caxiuanã (right) for both CTL (top) and TFE for the full experimental period.*

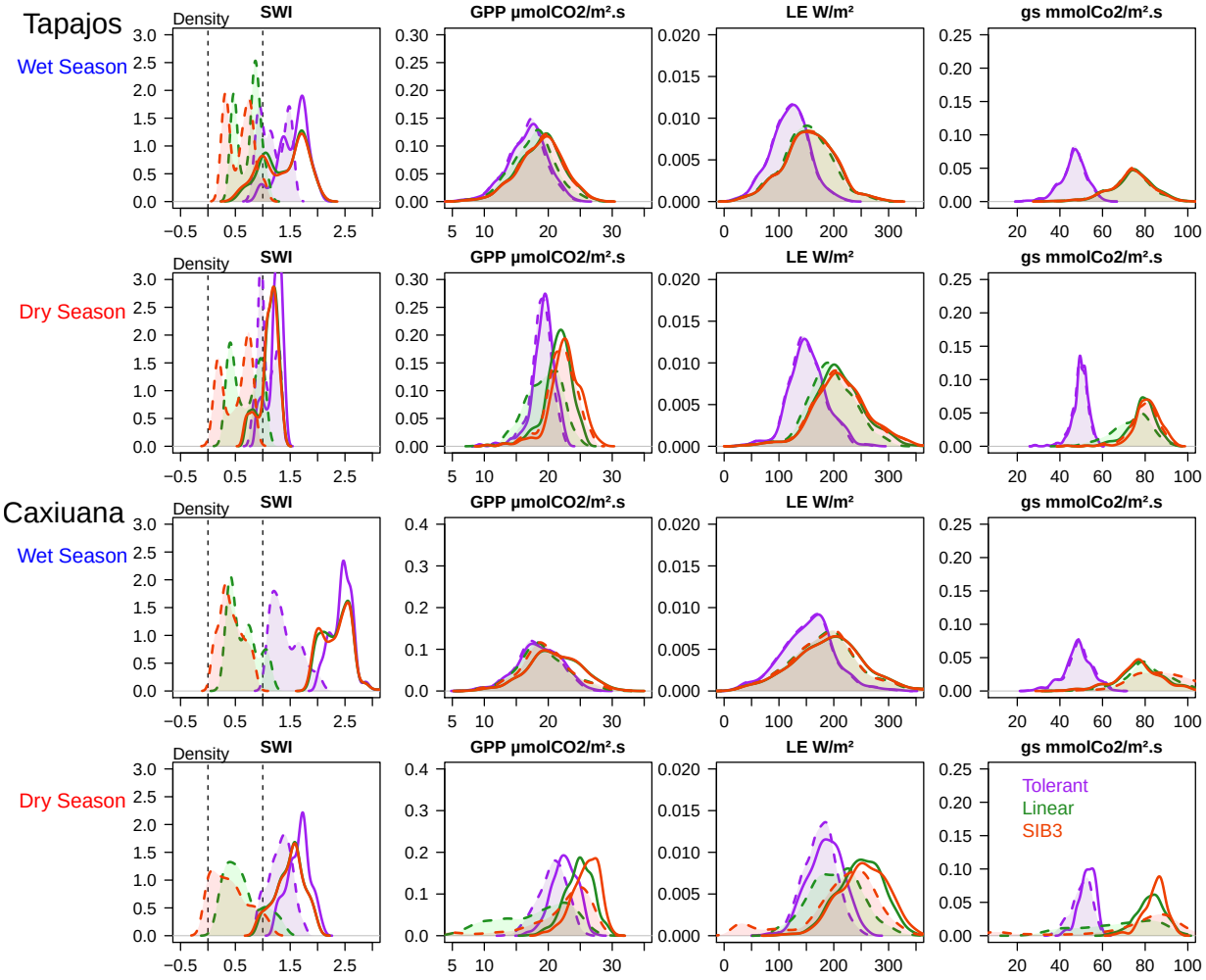

FIGURE 5 – *Probability density functions of the daily Soil Wetness Index (SWI), Gross Primary Production (GPP), Evapotranspiration (LE) and the stomatal conductance (Gs), for the Tolerant, Linear and SIB_3 WSF , calculated for the Dry season (from August to October) and the wet season (from February to April) during the treatment period (i.e. baseline year excluded) at Caxiuanã and Tapajós. Solid lines indicates the CTL plots and dashed lines and shaded areas the TFE plots. The daily means are calculated for incoming short wave radiation* $> 100\ W.m^{-2}$.

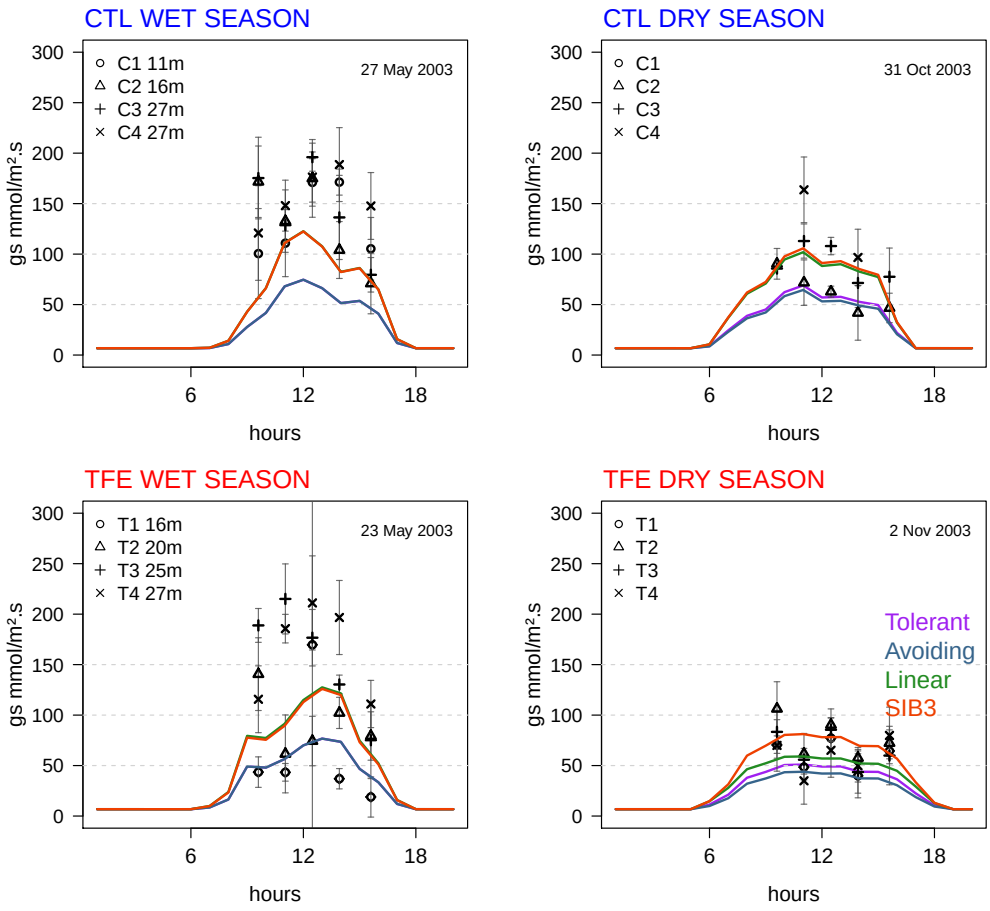

FIGURE 6 – *Seasonal variability of the diurnal cycle of stomatal conductance at Caxiuaña. Measurements were taken on 4 days at 4 different heigths in the canopy : C1-C4 designate trees in the CTL plot and T1-T4 trees the TFE plots and simulated g_s with the 4 WSF (lines) are representing the all canopy*

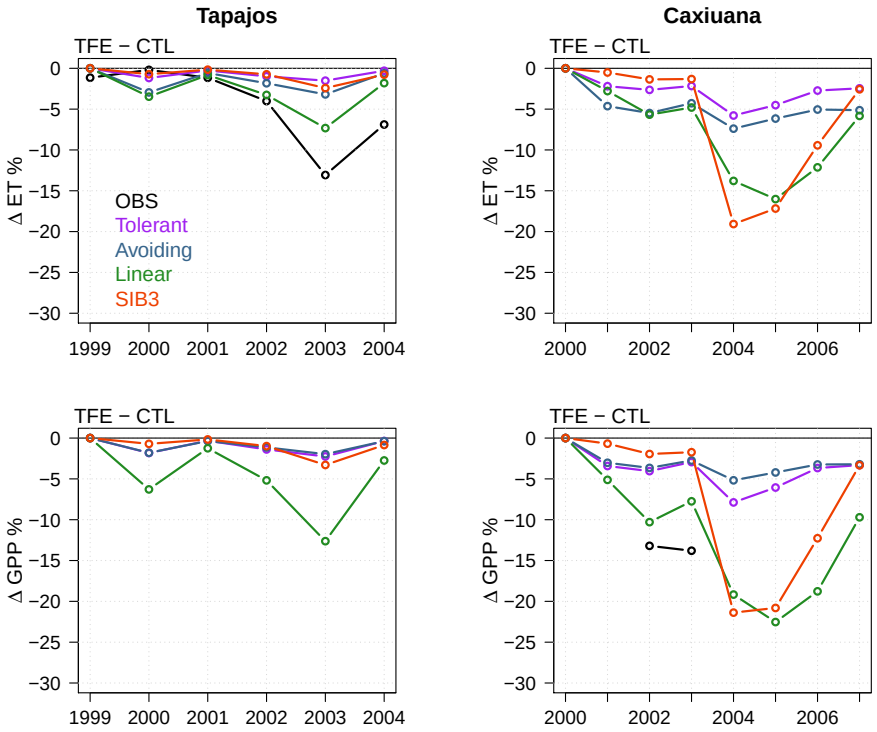

FIGURE 7 – *Annual mean differences (TFE plot minus CTL plot) in simulated ET (top) with $ISBA_{CC}$ and Markewitz's model outputs as proxy (Markewitz et al 2010). Annual differences (exclusion plot minus control plot) in simulated GPP (bottom) with $ISBA_{CC}$ and SPA's model outputs as proxy (Fisher et al 2007).*

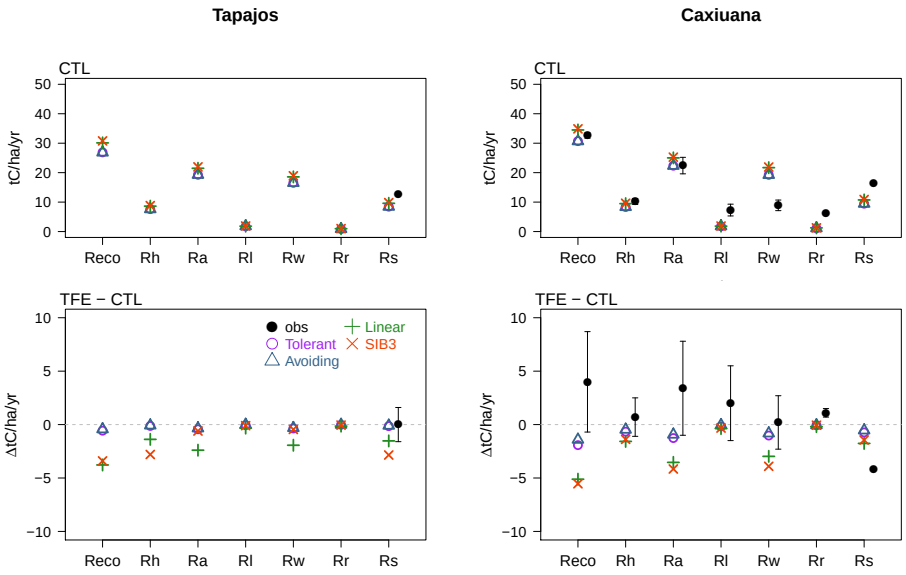

FIGURE 8 – *Annual Ecosystem (R_e), Heterotrophic (R_h), Autotrophic (R_a), Leaf (R_l), Wood (R_w) , Root (R_r) and Soil (R_s) Respirations for the fourth year of the experiment for the control plot (top) and the difference between the exclusion and control plot (bottom) at Tapajós (left) and Caxiuanã (right).*

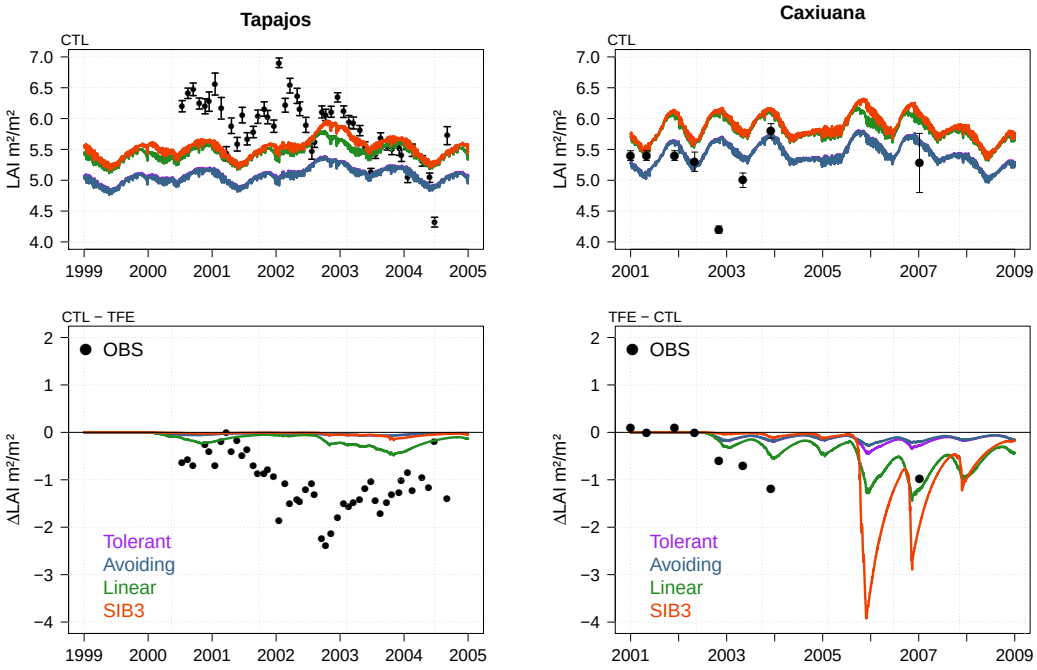

FIGURE 9 – *Times series of the daily Leaf Area Index (LAI) for the control plot (top) and the difference between the exclusion and control plot (bottom) at Tapajós (left) and Caxiuanã (right).*

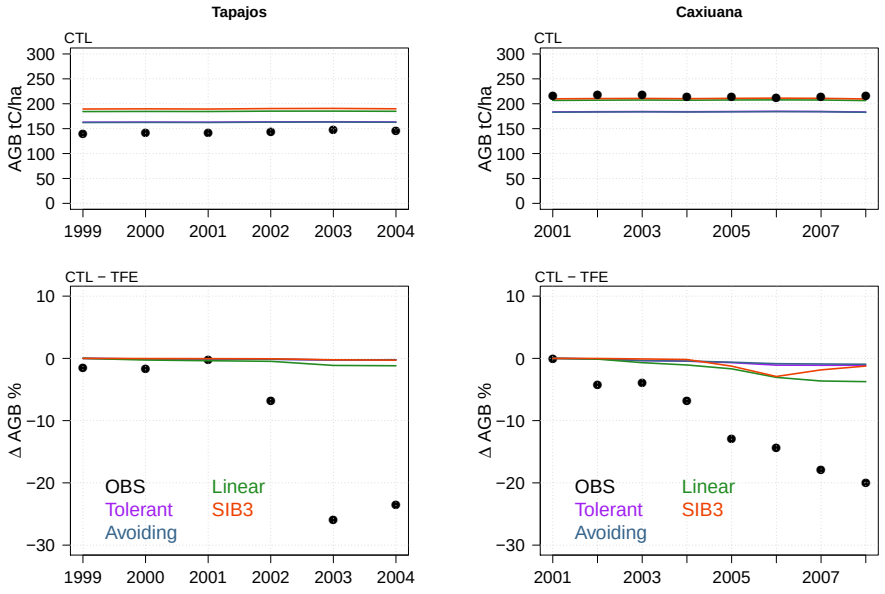

FIGURE 10 – *Times series of the yearly Above Ground Biomass (AGB) for the control plot (top) and the difference between the exclusion and control plot (bottom) at Tapajós (left) and Caxiuanã (right).*

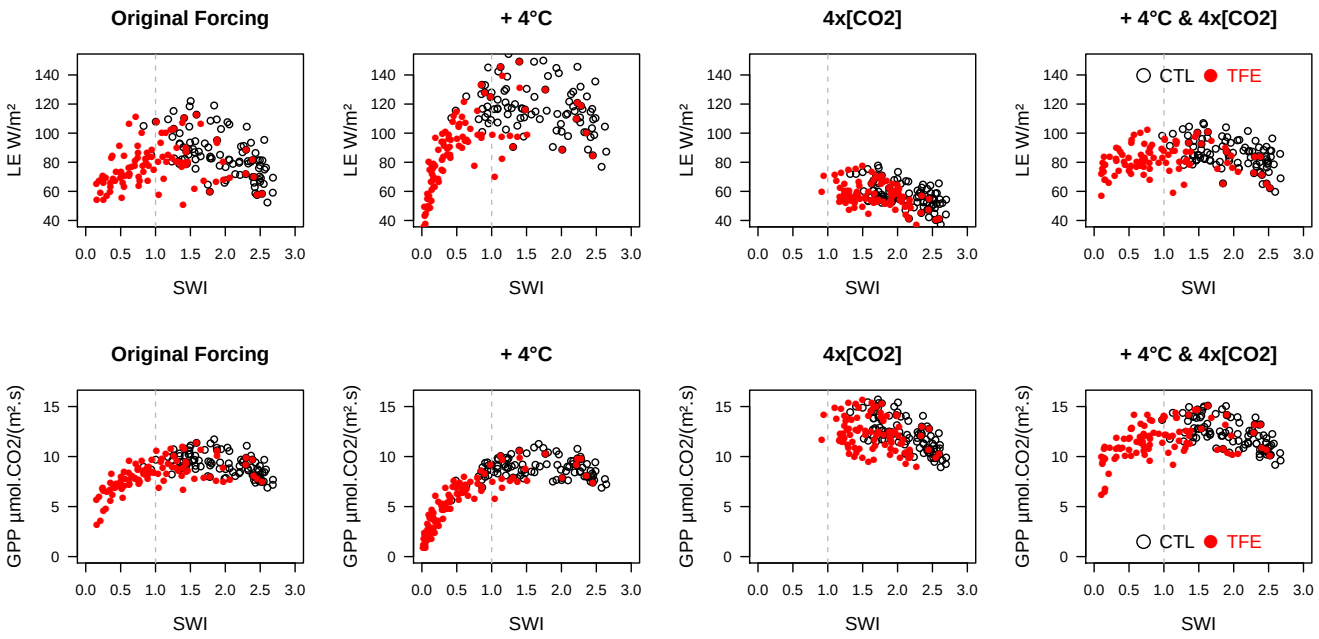

FIGURE 11 – *Simulated monthly LE and GPP vs monthly SWI using the Linear WSF, under undisturbed and disturbed meteorological forcings for both CTL (black empty dots) and TFE (red full dots) plots at Caxiuanã.*